

A Rhomboid-shaped Printed Monopole Antenna for Wideband Circular Polarization

Zaw Myo Lwin¹, Thae Su Aye²

Abstract: This paper presents the design of a wideband circularly-polarized printed monopole antenna with a rhomboid shape. The rhomboid-shaped patch is fed by a microstrip line offset from the center to generate circular polarization (CP). The ground plane configuration is optimized for wide bandwidth operation. Bandwidth (satisfying both 10-dB return loss and 3-dB axial ratio) of 76% (1.92 – 4.27 GHz) is achieved in this research. The size of the proposed antenna is $0.386\lambda_0^2$ (55×66 mm²) where λ_0 is the free space wavelength which corresponds to the center frequency of the bandwidth. The antenna has a fractional bandwidth-size ratio (BW/size) of 1.97 which is higher than most CP monopole antennas in the literature. This antenna is suitable for Wi-Fi, WiMAX, and other wireless applications which outperform using circular polarization.

Keywords: Circular polarization, Printed monopole antenna, Rhomboid shape, Wideband antenna

1 Introduction

Circularly-polarized (CP) antennas are more attractive than linearly-polarized antennas because of their ability to overcome fading, mitigate the Faraday rotation effect, and provide a nearly-fixed received signal level irrespective of the antenna position [1]. Therefore, they are preferable in many wireless communication systems such as RFID, GPS, WiFi, and WiMAX. Not only for wide bandwidth performance, but also for compactness, low cost, lightweight, and easy implementation, printed monopole antennas are desirable [2 – 3]. Therefore, printed monopole antennas with wideband circular polarization have attracted a lot of interest.

Some research on CP printed antennas with different shapes has been carried out in the literature [4 – 10] for wide bandwidth operation covering both 10-dB return loss and 3-dB axial ratio. Asymmetric arrangement of the two rectangular

¹Department of Electronic Engineering, Technological University (Kyaukse), Mandalay Division, Myanmar; Email: zawmyolwinn@gmail.com

²Faculty of Electronic Engineering, University of Technology (Yatanarpon Cyber City), Pyin Oo Lwin, Myanmar; Email: thaesuaye1483@gmail.com

radiators with regard to the feed line is proposed in [4] for wideband operation of 77.6%. The asymmetrically-fed rectangular patch and the modified ground plane in [5] produce a bandwidth of 51.4%. Panahi et al. [6] propose a CP antenna using the triangular patch and the triangular ground plane with 58.7% bandwidth. The printed monopole antenna with a moon shape and the optimized ground plane is designed in [7] and a bandwidth of 49% is achieved. The chifre-shaped patch and the rectangular ground through an asymmetric feeding is proposed in [8] and the bandwidth is 41.6%. In [9], the elliptical patch is fed asymmetrically with respect to the feed line, and the ground plane is modified for a wide bandwidth performance of 83.6%. The C-shaped radiator and the modified ground plane in [10] enable broad bandwidth of 97.7%.

All of these antennas [4 – 10] are based on asymmetric feeding with a relatively simple configuration using different patch shapes. However, in the literature, there has been no report on a wideband CP printed monopole antenna with a rhomboid shape. In this paper, a simple rhomboid patch is fed by a 50 Ω microstrip line asymmetrically to generate two electric fields with equal amplitude and 90° phase difference required for the circular polarization. Furthermore, the dimensions and placement of the ground plane with respect to the feed line and the patch are optimized for a wide bandwidth operation. Simulation results using FEKO software and return loss measurement results are shown to ascertain the antenna performance.

2 Antenna Design

The design procedure of the proposed antenna is illustrated in Fig. 1. A conventional asymmetrically-fed rectangular monopole antenna (Ant.1) generates two orthogonal electric fields enabling circular polarization. However, as shown in Fig. 2, its 3-dB axial ratio (AR) bandwidth is narrow. In Ant.2, the patch, the microstrip feed line, and the ground plane are tilted to form a rhomboid-shaped monopole antenna, and it is found that 3-dB AR bandwidth becomes wider than Ant.1. Finally, in Ant.3, two different stubs are embedded on the left and right sides of the ground plane to further enhance the 3-dB AR bandwidth. According to Fig. 2, it is quite obvious that the final design has the widest 3-dB AR bandwidth.

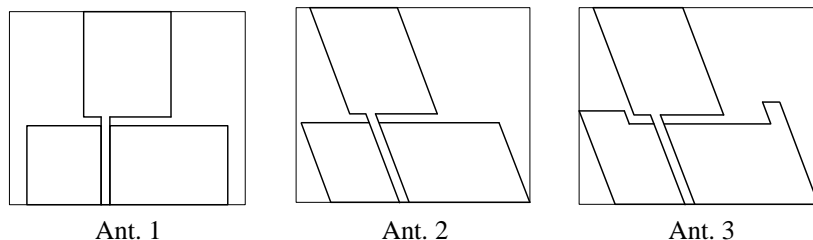


Fig. 1 – Design procedure of the proposed antenna.

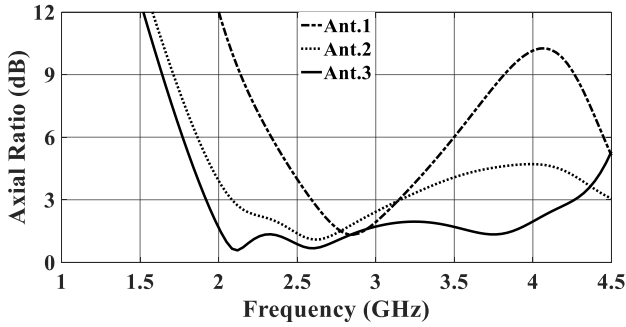


Fig. 2 – Simulated axial ratio comparison for three antenna configurations.

The configuration of the proposed antenna (Ant.3) is illustrated in Fig. 3. The patch geometry is a rhomboid with width $A = 28$ mm, length $B = 32.47$ mm, and tilted angle $\theta = 22.5^\circ$. The patch is fed asymmetrically by a 3 mm-wide microstrip line which is positioned at $d = 7$ mm offset from the left edge of the patch. The left and right edges of the ground plane are tilted at an angle θ and have lengths of $U_1 = 28.14$ mm and $U_2 = 30.31$ mm respectively. The dimensions of the left and right stubs on the ground plane are $p = 13.6$ mm, $q = 3.24$ mm, $r = 3.9$ mm and $s = 5.41$ mm. The bottom width of the ground plane is $V = 55.23$ mm. The gaps between the patch and the ground plane are $g_L = 1.5$ mm, $g_R = 8.25$ mm, and $g = 2$ mm. The substrate material used is FR4 with a relative permittivity of 4.4, loss tangent of 0.02, and the thickness h of 1.6 mm. The overall size of the antenna is $L_1 \times L_2$ (55×66 mm).

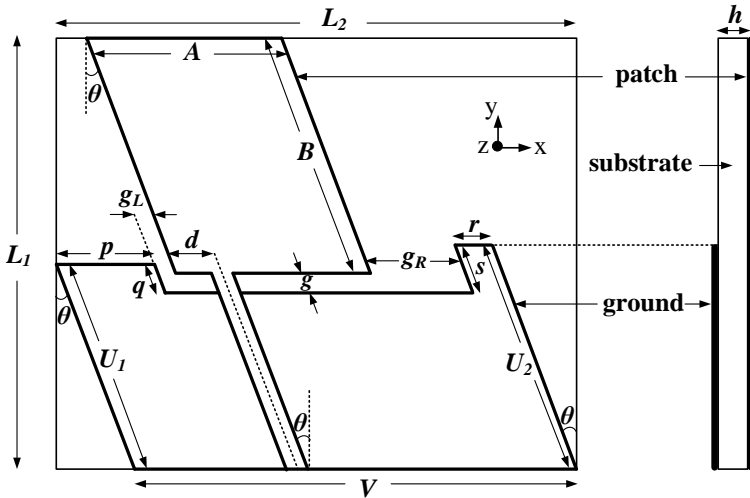


Fig. 3 – Structure of the proposed antenna.

3 Principle of Operation

To prove the circular polarization property of the proposed antenna, electric current distributions at four time instants are discussed in this section. Simulated electric current distributions for the operating frequency of 2.46 GHz are depicted in Figs. 4a – 4d for four time instants at $\omega t = 0^\circ$, 90° , 180° , and 270° respectively. At $\omega t = 0^\circ$, electric currents on the right side of the ground plane flow in opposite directions canceling out the radiation due to them. Therefore, in this case, electric currents on the patch and the left side of the ground plane, flowing towards the top right direction, produce radiation. At $\omega t = 90^\circ$, electric currents on both the rhomboid patch and the ground plane flow in the same direction, that is, to the top left. Thus, these currents are the sources of electric field radiation.

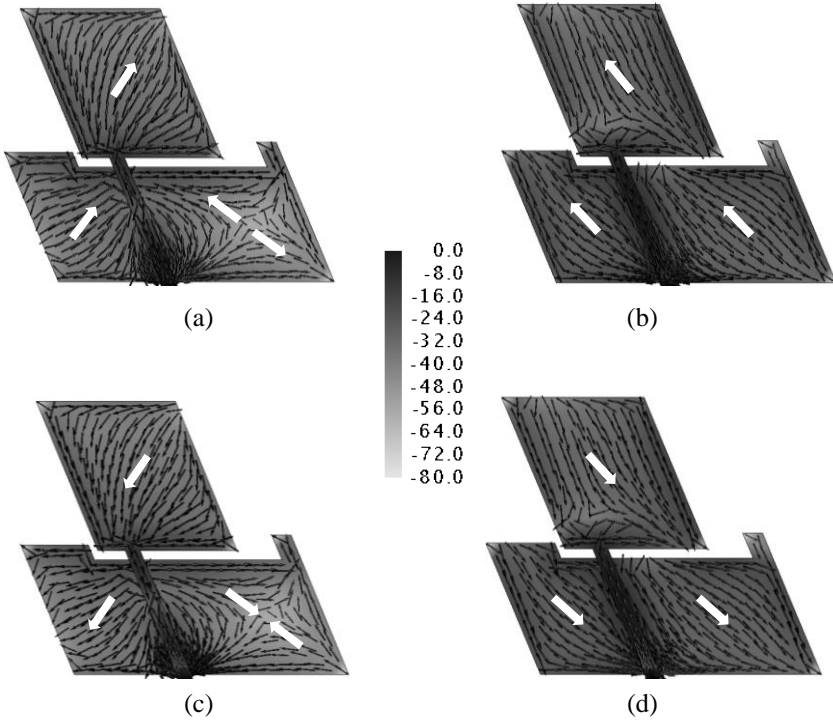


Fig. 4 – Electric current distributions [dB] at 2.46 GHz:
(a) $\omega t = 0^\circ$; (b) $\omega t = 90^\circ$; (c) $\omega t = 180^\circ$ and (d) $\omega t = 270^\circ$.

Similarly, the radiation due to the electric currents on the right side of the ground plane cancels out each other at $\omega t = 180^\circ$ because they flow in opposite directions. Radiation is generated by the electric currents on the patch and the left side of the ground plane which flow to the bottom left direction. At $\omega t = 270^\circ$, being in the bottom right direction, electric currents on the patch and the ground plane contribute to the electric field radiation. It can be seen that the electric field

rotates with time in the counterclockwise direction. Four time instants are chosen at 90° intervals and the directions of the electric field radiated at each instant are 90° apart. Therefore, a right hand circularly-polarized (RHCP) wave is generated in the positive z direction.

4 Parametric Study

This section discusses how various parameters affect the return loss and the axial ratio bandwidth. As shown in Figs. 5a and 5b, as the patch width A becomes less than 28 mm, although return loss gets better, the axial ratio worsens. However, when A is greater than 28 mm, both return loss and axial ratio deteriorate. Therefore, antenna width A of 28 mm is the optimum choice.

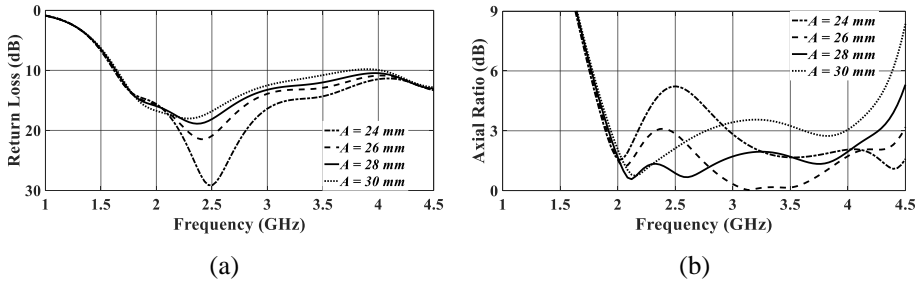


Fig. 5 – Simulated return losses (a) and axial ratios (b) for different widths A ($B = 32.47$, $\theta = 22.5^\circ$, $d = 7$, $U_1 = 28.14$, $U_2 = 30.31$, $V = 55.23$, $g_L = 1.5$, $g_R = 8.25$, $g = 2$, $q = 3.24$, $s = 5.41$, $L_1 = 55$, $L_2 = 66$, unit: mm).

Figs. 6a and 6b depict plots of return loss and axial ratio for the changes of the tilted angle θ . The larger the angle θ , the wider the axial ratio bandwidth and the worse the return loss performance. Regarding not only return loss but also axial ratio, the best value for the inclination angle θ is 22.5° . It is worth mentioning that the angle θ is one of the critical parameters of the proposed antenna design.

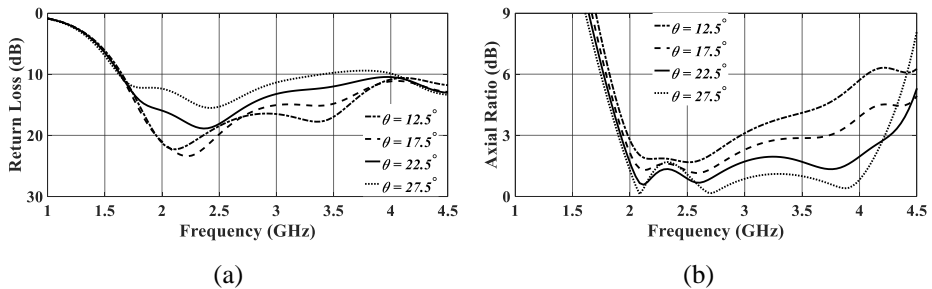


Fig. 6 – Simulated return losses (a) and axial ratios (b) for different tilted angles θ ($A = 28$, $B = 32.47$, $d = 7$, $g_L = 1.5$, $g_R = 8.25$, $g = 2$, $p = 13.6$, $r = 3.9$, unit: mm).

The position d of microstrip feed line is varied between the center and the left side of the patch and its effect on the antenna performance is investigated in Fig. 7a and 7b. Noting that the position d of 7 mm is halfway between the center and the left side of the patch, moving the feed line away from the left or right side of this point makes the axial ratio worse and worse. Thus, the asymmetrical placement of the microstrip feed line with respect to the patch is an important condition for producing circular polarization and it is found that the optimum position d of the feed line is at a quarter of the total patch width A .

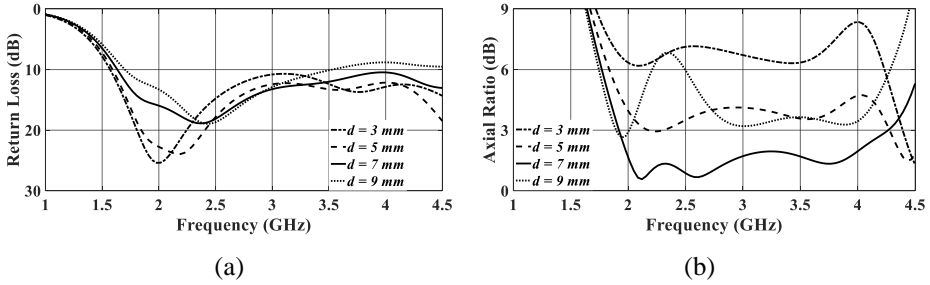


Fig. 7 – Simulated return losses (a) and axial ratios (b) for different feed positions d ($A = 28, B = 32.47, \theta = 22.5^\circ, U_1 = 28.14, U_2 = 30.31, V = 55.23, g_L = 1.5, g_R = 8.25, g = 2, p = 13.6, q = 3.24, r = 3.9, s = 5.41, L_1 = 55, L_2 = 66, \text{unit: mm}$).

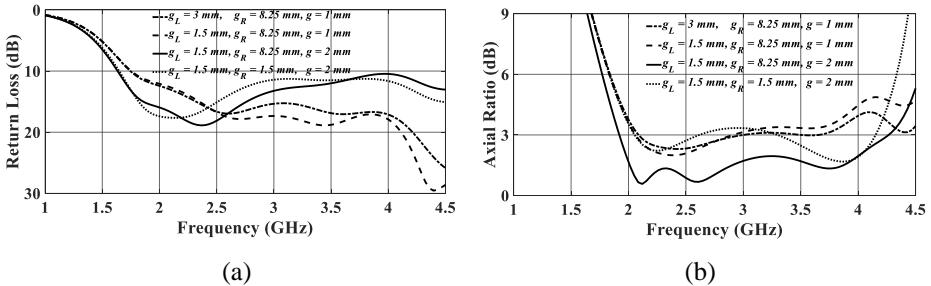


Fig. 8 – Simulated return losses (a) and axial ratios (b) for different gaps ($A = 28, B = 32.47, \theta = 22.5^\circ, d = 7, U_1 = 28.14, U_2 = 30.31, V = 55.23, q = 3.24, s = 5.41, L_1 = 55, L_2 = 66, \text{unit: mm}$).

Figs. 8a and 8b illustrate the return loss and the axial ratio for changing different gaps $g_L, g_R,$ and g . It can be seen that adjusting the gaps between the patch and the ground plane influences the return loss bandwidth. Each different combination of gaps gives a different performance and the optimum combination is found to be g_L of 1.5 mm, g_R of 8.25 mm, and g of 2 mm which gives a wide bandwidth in both return loss and axial ratio. Finally, dimensions q and s on the left and right stubs on the ground plane are varied in Figs. 9a and 9b. When both q and s are made equal at 3.24 mm, the axial ratio bandwidth is rather narrow. Moreover, if the length of q is longer than s , the antenna performance is bad.

When q is arranged to be shorter than s , the performance gets better. Both return loss and axial ratio bandwidth become wide at unequal lengths of $q = 3.24$ mm and $s = 5.41$ mm. On the whole, it is found that the parameters ($A, \theta, d, g_L, g_R, g, q, s$) have an influence on the return loss and the axial ratio, and hence the optimum design is achieved by carefully tuning them.

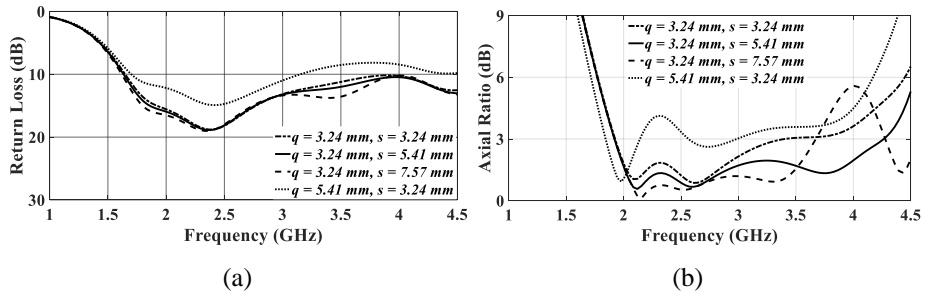


Fig. 9 – Simulated return losses (a) and axial ratios (b) for different stub dimensions ($A = 28, B = 32.47, \theta = 22.5^\circ, d = 7, V = 55.23, g_L = 1.5, g_R = 8.25, g = 2, p = 13.6, r = 3.9, L_1 = 55, L_2 = 66$, unit: mm).

5 Results and Discussions

Photographs of the fabricated antenna are depicted in Figs. 10a and 10b. The antenna was fabricated on the FR4 dielectric substrate material with a thickness of 1.6 mm using MITS Eleven Lab PCB prototyping machine.

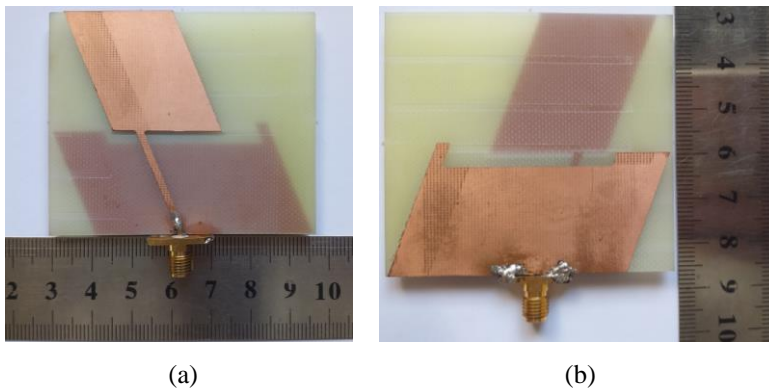


Fig. 10 – The fabricated antenna: (a) top view; (b) bottom view.

Fig. 11a illustrates a comparison of the simulated and measured return loss. The measurement was performed using Anritsu MS2038C vector network analyzer. The measured result almost agrees with the simulated return loss. A simulated axial ratio is depicted in Fig. 11b. Due to the lack of additional measurement equipment, the axial ratio of the proposed antenna could not be

measured. The simulated bandwidth (satisfying both 10-dB return loss and 3-dB axial ratio) of the proposed antenna is 76% (1.92 – 4.27 GHz).

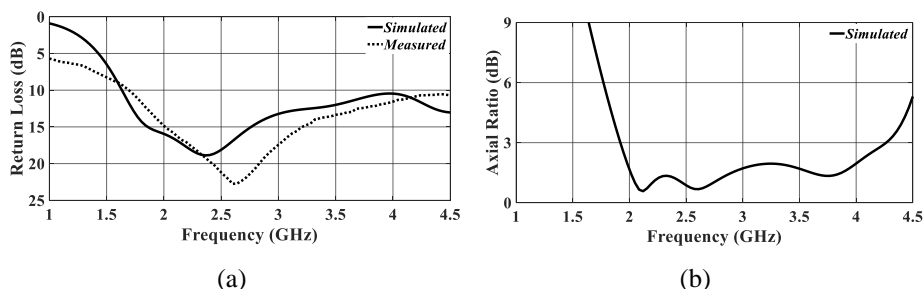


Fig. 11 – Simulated return loss (a) (also measured) and axial ratio (b).

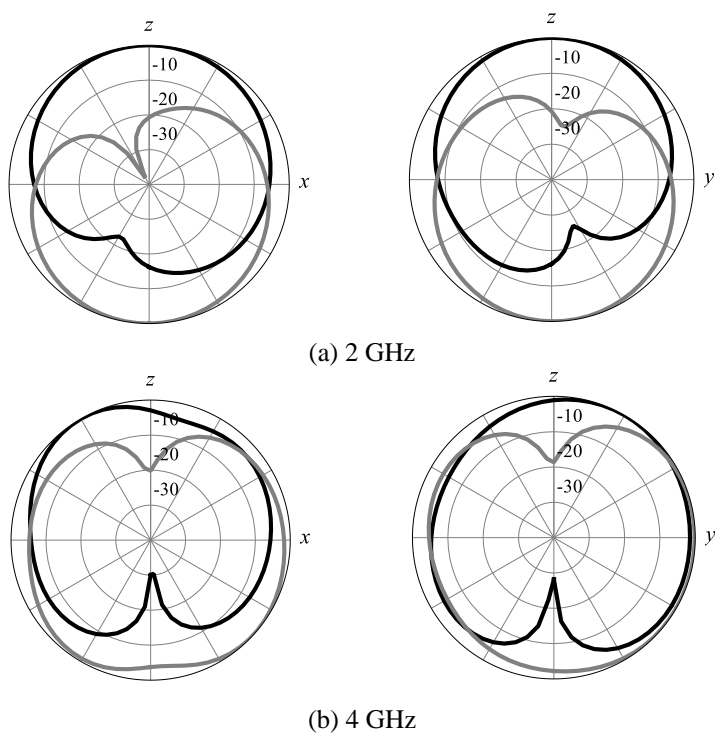


Fig. 12 – Normalized radiation patterns (black line: RHCP, gray line: LHCP, unit: dB).

Simulated normalized radiation patterns are illustrated in Figs. 12a and 12b for 2 GHz and 4 GHz respectively. Both right-hand circular polarization (RHCP) and left-hand circular polarization (LHCP) radiation patterns are shown on both x - z plane and y - z plane. According to the results, RHCP radiation occurs along the positive z direction and LHCP radiation along the negative z direction where

the positive z direction and the negative z direction correspond to the top side and bottom side of the antenna respectively.

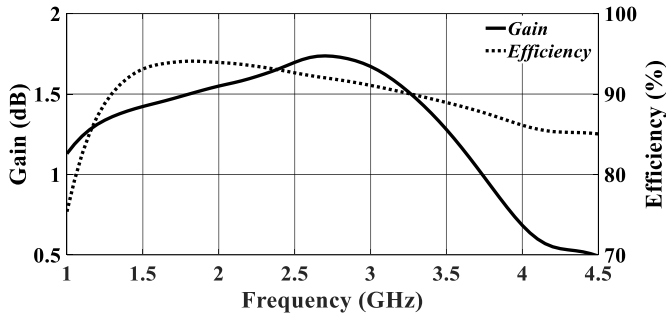


Fig. 13 – Simulated gain and efficiency at the positive z direction.

Table 1
Comparison of the CP monopole antennas

References	Bandwidth in GHz (10-dB return loss and 3-dB axial ratio)	Fractional BW	Size [mm ²]	Size [λ_0^2]	BW/size
[4]	1.5 – 3.4	0.776	72 × 148	0.711	1.09
[5]	1.82 – 3.08	0.514	70 × 70	0.327	1.57
[7]	2.28 – 3.76	0.49	70 × 46.58	0.331	1.48
[8]	1.98 – 3.02	0.416	58.4 × 63	0.256	1.63
[9]	2.2 – 5.36	0.836	50 × 60	0.476	1.76
[10]	2.25 – 6.55	0.977	49 × 55	0.58	1.68
[11]	5.91 – 8.55	0.365	22 × 16	0.205	1.78
[12]	5.15 – 7.1	0.318	20 × 20	0.166	1.92
[13]	3.95 – 6.57	0.498	50 × 50	0.769	0.65
[14]	4.4 – 7.6	0.533	46 × 40	0.736	0.72
[15]	4.28 – 8.42	0.652	25 × 25	0.28	2.33
[16]	4.25 – 5.95	0.333	52 × 55	0.827	0.4
[17]	2.3 – 4.5	0.647	50 × 55	0.353	1.83
[18]	2.05 – 3.95	0.633	55 × 50	0.275	2.3
[19]	2.38 – 4	0.508	44 × 44	0.219	2.32
[20]	4.28 – 7.44	0.539	30 × 32	0.366	1.47
[21]	5.91 – 10.58	0.566	30 × 25	0.566	1
[22]	3.6 – 6.84	0.621	60 × 60	1.09	0.57
[23]	2.4 – 6.6	0.933	49 × 51	0.562	1.66
Proposed	1.92 – 4.27	0.759	55 × 66	0.386	1.97

The simulated gain and radiation efficiency of the antenna are depicted in Fig. 13. Both gain and efficiency are simulated at the positive z direction. Although a maximum gain of 2.4 dB occurs around 2.7 GHz, with an increase in frequency after 3 GHz, the gain decreases dramatically. Approximately 88% radiation efficiency is achieved within a 1.92 – 4.27 GHz frequency span. Efficiency of the proposed antenna also declines as the frequency increases.

As shown in **Table 1**, the proposed antenna is compared with some CP printed monopole antennas in order to evaluate its fractional bandwidth-size (BW/size) ratio. As for antenna performance, the wider bandwidth and the smaller size are always desirable. Therefore, the higher BW/size ratio, the better it is. For a fair comparison, only printed monopole antenna (PMA) types are selected from the literature, and printed slot antenna types are omitted because they provide inherently wider bandwidth than PMAs. The fractional bandwidth (BW) is calculated by dividing the bandwidth that satisfies both 10-dB return loss and 3-dB axial ratio by its center frequency. The size (area) of the antenna is expressed in terms of electrical size λ_0^2 where λ_0 is the free space wavelength which corresponds to the center frequency of the bandwidth. As seen from **Table 1**, the proposed antenna has a higher BW/size ratio than most CP monopole antennas except for references [15, 18, 19]. The proposed antenna has a fractional bandwidth of 0.759 and electrical size (area) of $0.386\lambda_0^2$ which gives BW/size ratio of 1.97.

6 Conclusion

In this paper, a wideband circularly-polarized antenna with a rhomboid shape was designed. The antenna structure was based on the asymmetrical placement of the rhomboid-shaped patch and the ground plane with respect to the microstrip feed line. Parametric studies were carried out to investigate the effect of the various parameters on the return loss and the axial ratio bandwidth. Due to the lack of a measurement facility, although the axial ratio, radiation pattern, and the gain of the antenna could not be measured, the return loss was measured and found to agree with the simulation result. In terms of the fractional bandwidth-size (BW/size) ratio, the antenna outperforms most of its CP counterparts with the value of 1.97. The wide bandwidth of 76% (satisfying both 10-dB return loss and 3-dB axial ratio) between the frequency span of 1.92 – 4.27 GHz is appropriate for several wireless communications systems with circular polarization.

7 References

- [1] S.S. Gao, Q. Luo, F. Zhu: Circularly Polarized Antennas, 1st Edition, Wiley-IEEE Press, Chichester, 2014.

A Rhomboid-shaped Printed Monopole Antenna for Wideband Circular Polarization

- [2] K.P. Ray: Design Aspects of Printed Monopole Antennas for Ultra-Wide Band Applications, *International Journal of Antennas and Propagation*, Vol. 2008, April 2008, ID 713858, pp. 1 – 7.
- [3] G. Bozdag, A. Kustepeli: Wideband Printed Planar Monopole Antenna for PCS, UWB and X-Band Applications, *Progress in Electromagnetics Research C*, Vol. 60, December 2015, pp. 95 – 103.
- [4] K.G. Thomas, G. Praveen: A Novel Wideband Circularly Polarized Printed Antenna, *IEEE Transactions on Antennas and Propagation*, Vol. 60, No. 12, December 2012, pp. 5564 – 5570.
- [5] T. Fujimoto, K. Jono: Wideband Rectangular Printed Monopole Antenna for Circular Polarisation, *IET Microwaves, Antennas & Propagation*, Vol. 8, No. 9, June 2014, pp. 649 – 656.
- [6] A. Panahi, X. L. Bao, G. Ruvio, M.J. Ammann: A Printed Triangular Monopole with Wideband Circular Polarization, *IEEE Transactions on Antennas and Propagation*, Vol. 63, No. 1, January 2015, pp. 415 – 418.
- [7] N. Benyang Hu, Z. Shen: Broadband Circularly-Polarized Moon-Shaped Monopole Antenna, *Microwave and Optical Technology Letters*, Vol. 57, No. 5, May 2015, pp. 1135 – 1139.
- [8] R.- C. Han, S.- S. Zhong: Broadband Circularly-Polarised Chifre-Shaped Monopole Antenna with Asymmetric Feed, *Electronics Letters*, Vol. 52, No. 4, February 2016, pp. 256 – 258.
- [9] T. Fujimoto, T. Ishikubo, M. Takamura: A Wideband Printed Elliptical Monopole Antenna for Circular Polarization, *IEICE Transactions on Communications*, Vol. E100-B, No. 2, February 2017, pp. 203 – 210.
- [10] H. Tang, K. Wang, R. Wu, C. Yu, J. Zhang, X. Wang: A Novel Broadband Circularly Polarized Monopole Antenna based on C-Shaped Radiator, *IEEE Antennas and Wireless Propagation Letters*, Vol. 16, 2017, pp. 964 – 967.
- [11] B. Chen, Y.- C. Jiao, F.- C. Ren, L. Zhang: Broadband Monopole Antenna with Wideband Circular Polarization, *Progress in Electromagnetics Research Letters*, Vol. 32, May 2012, pp. 19 – 28.
- [12] S. Ahdi Rezaeieh, A. Abbosh, M.A. Antoniades: Compact CPW-Fed Planar Monopole Antenna with Wide Circular Polarization Bandwidth, *IEEE Antennas and Wireless Propagation Letters*, Vol. 12, September 2013, pp. 1295 – 1298.
- [13] T.T. Le, H.C. Park: Very Simple Circularly Polarised Printed Patch Antenna with Enhanced Bandwidth, *Electronics Letters*, Vol. 50, No. 25, December 2014, pp. 1896 – 1898.
- [14] K. Ding, T. Yu, D. Qu, C. Peng: Broadband CPW-Fed Circularly Polarized Falcate-Shaped Monopole Antenna for UWB Applications, *Frequenz*, Vol. 68, No. 7-8, July 2014, pp. 305 – 312.
- [15] K. Ding, C. Gao, T. Yu, D. Qu: Broadband C-Shaped Circularly Polarized Monopole Antenna, *IEEE Transactions on Antennas and Propagation*, Vol. 63, No. 2, February 2015, pp. 785 – 790.
- [16] T.V. Hoang, T.T. Le, H.C. Park: Bandwidth Improvement of a Circularly Polarised Printed Monopole Antenna Using a Lumped Capacitor, *Electronics Letters*, Vol. 52, No. 13, June 2016, pp. 1091 – 1092.
- [17] K. Ding, C. Gao, Y. Wu, D. Qu, B. Zhang: A Broadband Circularly Polarized Printed Monopole Antenna with Parasitic Strips, *IEEE Antennas and Wireless Propagation Letters*, Vol. 16, July 2017, pp. 2509 – 2512.
- [18] K. Ding, Y.- X. Guo, C. Gao: CPW-Fed Wideband Circularly Polarized Printed Monopole Antenna with Open Loop and Asymmetric Ground Plane, *IEEE Antennas and Wireless Propagation Letters*, Vol. 16, 2017, pp. 833 – 836.

- [19] Md. Samsuzzaman, M.T. Islam, M.J. Singh: A Compact Printed Monopole Antenna with Wideband Circular Polarization, *IEEE Access*, Vol. 6, September 2018, pp. 54713 –54725.
- [20] M. Midya, S. Bhattacharjee, M. Mitra: Broadband Circularly Polarized Planar Monopole Antenna with G-Shaped Parasitic Strip, *IEEE Antennas and Wireless Propagation Letters*, Vol. 18, No. 4, April 2019, pp. 581 –585.
- [21] P. Chaudhary, A. Kumar: Compact Ultra-Wideband Circularly Polarized CPW-Fed Monopole Antenna, *AEU - International Journal of Electronics and Communications*, Vol. 107, July 2019, pp. 137 –145.
- [22] U. Banerjee, A. Karmakar, A. Saha, P. Chakraborty: A CPW-Fed Compact Monopole Antenna with Defected Ground Structure and Modified Parasitic Hilbert Strip Having Wideband Circular Polarization, *AEU - International Journal of Electronics and Communications*, Vol. 110, October 2019, pp. 1 –9.
- [23] B.- H. Xu, Y. Zhao, L. Gu, C. Huang, Z. Nie: Broadband Circularly Polarized Printed Falcate-Shaped Monopole Antenna, *International Journal of RF and Microwave Computer-Aided Engineering*, Vol. 30, No. 11, November 2020, pp. 1 –12.